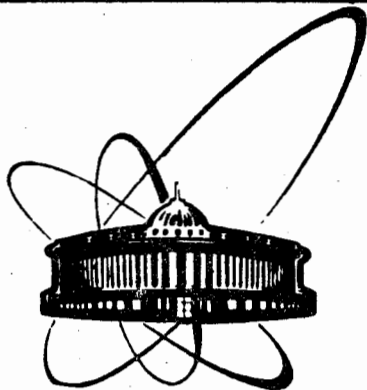


89-444



ОБЪЕДИНЕННЫЙ  
ИНСТИТУТ  
ЯДЕРНЫХ  
ИССЛЕДОВАНИЙ  
ДУБНА

K42

E4-89-444

M. Kh. Khankhasayev

UNITARY SCATTERING THEORY  
OF LOW-ENERGY PIONS BY LIGHT NUCLEI:  
APPLICATIONS

Submitted to "Nuclear Physics A"

1989

Ханхасаев М.Х.

E4-89-444

Унитарная теория рассеяния пионов  
низких энергий на легких ядрах: приложения

Представлены результаты единого описания экспериментальных данных по упругому рассеянию пионов и пион-атомных данных для ядер  ${}^4\text{He}$ ,  ${}^{12}\text{C}$  и  ${}^{16}\text{O}$  в рамках унитарного подхода. Показано сильное влияние канала поглощения пиона на канал упругого рассеяния. Получен единый набор параметров поправки на поглощение, обеспечивающий количественное описание данных по упругому рассеянию при энергиях 0 - 50 МэВ.

Работа выполнена в Лаборатории теоретической физики ОИЯИ.

Препринт Объединенного института ядерных исследований. Дубна 1989

Khankhasayev M.Kh.

E4-89-444

Unitary Scattering Theory of Low-Energy  
Pions by Light Nuclei: Applications

The results of a unified description of both the low-energy scattering data and the pionic atom data for  ${}^4\text{He}$ ,  ${}^{12}\text{C}$  and  ${}^{16}\text{O}$  within the framework of the UST-approach are presented. Strong influence of the pion absorption on the elastic scattering channel at low energies is demonstrated. It is shown that a unique set of parameters of the absorption correction fitted to pionic atom data provides good quantitative description of the pion elastic scattering data at energies up to 50 MeV.

The investigation has been performed at the Laboratory of Theoretical Physics, JINR.

Preprint of the Joint Institute for Nuclear Research. Dubna 1989

## 1. Introduction

The interaction of low - energy pions (below  $\sim 70$  MeV ) with nuclei has attracted much attention in the last decade. It has been stimulated by a systematic study of pion-nucleus reactions at the existing meson factories in this energy range. The scattering data supplemented by the pionic atom data provide a good basis for testing the theory of pion - nucleus interaction.

The present paper is aimed to describe systematically the results of the analysis of the elastic scattering of low-energy pions by the light nuclei  ${}^4\text{He}$ ,  ${}^{12}\text{C}$  and  ${}^{16}\text{O}$  in the framework of the unitary scattering theory (UST). The formalism of the UST approach has been presented in several earlier papers /1-3/ ( see especially ref. / 1 / which we shall refer throughout the present paper as Part 1 ).

The UST-approach is based on unconventional formulation of the quantum scattering theory in which the evolution of the system with respect to the coupling constant is considered /4/.

We systematically examine here the problem of a unified description of both the low-energy scattering data and the pionic atom data. First particular results of this approach have been published in a recent letter /5/ . Since this letter new experimental results on the elastic scattering of  $\pi^-$ -mesons by  ${}^{12}\text{C}$  and  ${}^{16}\text{O}$  at 20, 30 and 50 MeV /6,7/ and on the total reaction cross section at 50 and 65 MeV /8/ became available. We analyze these data in the present paper too.

Our paper is organized as follows. In sect.2 we make a sketch of the calculational scheme of the UST-approach. In sect.3 we discuss the determination of the absorption parameters from the pionic atom data. The results of the description of the scattering data are presented in sect.4. The strong interaction shift and width in the 2p-level of the pionic helium have been deduced from

ОБЪЕДИНЕННЫЙ ИНСТИТУТ  
ЯДЕРНОЙ ФИЗИКИ  
СВЯТОГО ПЕТРА

the analysis of the low energy  $\pi - {}^4\text{He}$  scattering data. In the concluding section 5 we summarise the main results of our study.

## 2. Formalism of the unitary approach

Referring to the details to ref./1/, we outline only the basic elements of the UST approach. The characteristic feature of this method is that a formalism is developed for a direct calculation of the pion-nucleus phase shifts.

The general formula for the  $\pi$ -nucleus phase shifts is of the form

$$\delta_{\pi A}(k) = \delta_{\pi A}^{\text{pot}}(k) + \delta_{\pi A}^{\text{abs}}(k). \quad (2.1)$$

Here,  $\delta_{\pi A}^{\text{pot}}$  is the phase shift caused by the pure potential scattering and  $\delta_{\pi A}^{\text{abs}}$  is the absorption correction.

**2.1.  $\delta_{\pi A}^{\text{pot}}$ .** In Part 1 we developed an iterative method for solving the basic equations for this quantity appropriate for the study of interaction of low-energy pions with light nuclei. We determined the range of convergence of the iterative series (below  $\sim 70$  MeV). At these energies it is sufficient to take into account only two lowest iterations. It has been shown that  $\delta_{\pi A}^{\text{pot}}$  is expressed in terms of the  $\pi N$ -phase shifts, nuclear form factors and correlation functions.

In our calculations we use for  ${}^4\text{He}$ ,  ${}^{12}\text{C}$  and  ${}^{16}\text{O}$  the form factors, correlation functions and single-particle density calculated in the harmonic oscillator model. The nuclear size parameters are determined from the scattering data<sup>9/</sup>. For the  $\pi N$ -phase shifts we employ the parametrization according to Row, Solomon and Landau /10/. The off-shell behaviour of the  $\pi N$  u-matrix is described using a rank-one separable potential with the form factor in the form

$$g_{\nu}(k) = k^{\ell} / (k^2 + \beta^2)^{\ell+1} \quad (2.2)$$

with  $\beta_{\nu} = 2.11 \text{ fm}^{-1}$  quite fairly describing the  $\pi N$  phase shifts of ref./10/.

**2.2.  $\delta_{\pi A}^{\text{abs}}$ .** The absorption correction ( see eqs.(6.2) and (6.3) in Part 1) for the nuclei with both zero spin and isospin reads as

$$\delta_{\pi A, \ell}^{\text{abs}} = A(A-1)k \frac{1+\xi}{1+2\xi/A} (\hat{\rho}_{\ell}^2(k) [\bar{B}_0(k) + \alpha \cdot k^2 \cdot \bar{C}_0(k)] + \beta \cdot k^2 \cdot \bar{C}_0(k) [(\ell+1)\hat{\rho}_{\ell+1}^2(k) + \ell \hat{\rho}_{\ell-1}^2(k)] / (2\ell+1)), \quad (2.3)$$

where  $\hat{\rho}_{\ell}^2$  is the partial wave of  $\hat{\rho}^2(q)$ , and  $\alpha$  and  $\beta$  are the angular transformation parameters:  $\alpha = -\xi(1-2/A)(1+\xi/2A)/(1+\xi)^2$ ,  $\beta = (1+\xi/2A)/(1+\xi)$ .

At low energies the complex parameters  $\bar{B}_0$  and  $\bar{C}_0$  we determine from the experimental data on the  $\pi$ -nucleus scattering lengths ( $a_0 = \lim_{k \rightarrow 0} \delta_0(k)/k$ ) and volumes ( $a_1 = \lim_{k \rightarrow 0} \delta_1(k)/k^3$ ):

$$\begin{aligned} a_0^{\text{exp}} - a_0^{\text{pot}} &= \gamma \cdot \hat{\rho}_0^2(0) \cdot \bar{B}_0, & \gamma &= A(A-1)(1+\xi)/(1+\xi/2A), \\ a_1^{\text{exp}} - a_1^{\text{pot}} &= \gamma \cdot [\bar{B}_0 \cdot \delta + \bar{C}_0 \cdot \beta \cdot \hat{\rho}_0^2(0)/3], \end{aligned} \quad (2.4)$$

where  $\delta = \lim_{k \rightarrow 0} \hat{\rho}_1^2(k)/k^2$ . The quantities  $a_{0,1}^{\text{pot}}$  are calculated in the framework of the potential theory.

One can expect that the parameters  $\bar{B}_0$  and  $\bar{C}_0$  corresponding to the short range part of the  $\pi$ -nucleus interaction are approximately constant in the low energy domain 0 - 50 MeV. In ref./11/, this has been demonstrated by the example of the  $\pi$ - ${}^4\text{He}$  scattering, and the calculations presented below confirm that conclusion.

**2.3. Coulomb effects.** The procedure of taking into account the Coulomb interaction has been described in sect.7 of Part 1. The charge form factors for  ${}^4\text{He}$ ,  ${}^{12}\text{C}$  and  ${}^{16}\text{O}$  are taken in the Gaussian form

$$F_A^{\text{ch}}(q^2) = (1 - 4\alpha Z) \exp(-Z), \quad Z^2 = q^2 a_{\text{ch}}^2 / 4, \quad \alpha = (A-4)/6A. \quad (2.5)$$

The charge distribution parameter  $a_{\text{ch}}$  is expressed through the charge radius  $R_{\text{ch}} = \langle r^2 \rangle_A^{1/2}$  of the nucleus by the equation

$$a_{\text{ch}}^2 = \frac{2}{3} \left( \frac{3A}{5A-8} \right) R_{\text{ch}}^2, \quad (2.6)$$

following from the definition:  $F_{\text{ch}}(q^2) = 1 - q^2 R_{\text{ch}}^2 / 6$ , as  $q^2 \rightarrow 0$ .

The charge form factor of the pion is taken in the form <sup>/12/</sup>

$$F_{\pi}^{\text{ch}}(q^2) = (1 + q^2/M_V^2), \quad M_V = 0.462(2) \text{ (GeV/c)}^2. \quad (2.7)$$

This value of  $M_V$  corresponds to the charge radius of the pion  $\langle r_{\pi}^2 \rangle^{1/2} = 0.711(9) \text{ fm}$ .

### 3. Absorption parameters and pionic atoms

In this section we consider the problem of determining the parameters  $\tilde{B}_0$  and  $\tilde{C}_0$  of the absorption correction  $\delta_{\pi A}^{\text{abs}}$  from the pionic atom data using the system of eqs. (2.4).

Recently <sup>/13-14/</sup> measurements of the 1s- and 2p-energy level shifts and widths in the  $\pi^-$ -atoms of  $^{12}\text{C}$  and  $^{16}\text{O}$  have been performed. We collect these data in table.1. For pionic helium only the 1s-energy level shift and width are measured <sup>/16/</sup>. Below, we shall determine the 2p-level characteristics in the pionic helium from the low-energy scattering data.

Table 1. Strong interaction shifts and widths in the 1s - and 2p- energy levels in pionic atoms

Nucleus	$\epsilon_{1s}, \text{KeV}$	$\Gamma_{1s}, \text{KeV}$	$\epsilon_{2p}, \text{eV}$	$\Gamma_{2p}, \text{eV}$	Refs.
$^4\text{He}$	-0.0757(20)	0.045(3)	-	$7.2(3.3) \times 10^{-4}$	/16/
$^{12}\text{C}$	-5.822(55)	2.77(4)	-	1.17(11)	/13/
	-	-	3.16(16)	1.36(22)	/14/
$^{16}\text{O}$	-15.43(10)	7.92(32)	-	4.82(36)	/15/
	-	-	15.05(26)	6.77(36)	/14/

#### 3.1. Scattering lengths and volumes: experiment

There are two possibilities to obtain  $a_{0,1}^{\text{exp}}$  from the pionic atom data. The first is based on using the well-known DGBT-formula <sup>/17,18/</sup>

$$a_{\ell} = \frac{1}{c_{nl}} \frac{1}{z^2} n^{2\ell+4} [(2\ell)!!]^2 \frac{(n-\ell-1)!}{(n+\ell)!} \left( \frac{a_B}{2} \right)^{2\ell+1} \frac{\epsilon_{nl} + i\Gamma_{nl}/2}{E_c}, \quad (3.1)$$

where  $a_B = \hbar^2/M_{\pi A} e^2 \zeta$  is the first Bohr radius,  $E_c = M_{\pi A} \alpha^2$  is the Coulomb unity of energy ( $\alpha=1/137$ ),  $\zeta=Ze$  is the charge of the nucleus,  $M_{\pi A}$  is the reduced mass of the  $\pi$ -nucleus system. The coefficients  $c_{nl}$  takes into account the charge distribution in the nucleus. For the 1s-state  $c_{1s}$  can be parameterized with a good accuracy by the simple formula <sup>/19/</sup>

$$c_{1s} = 1 - 0.02 A, \quad (3.2)$$

where  $A$  is the mass number. More exact expression for  $c_{1s}$  presented in ref. <sup>/20/</sup> gives results which are numerically close to (3.2). For the considered nuclei  $^4\text{He}$ ,  $^{12}\text{C}$  and  $^{16}\text{O}$  the parameter  $c_{2p} = 1.00, 1.05$  and  $1.07$ , i.e.  $c_{2p} \approx 1.0$ . These values are calculated numerically using the Klein-Gordon equation.

Table 2. Pion-nucleus scattering lengths and volumes: experimental values

Nucleus	$a_0^{\text{exp}}, \text{fm}$	$a_1^{\text{exp}}, \text{fm}^3$	Refs.
$^4\text{He}$	$-0.141(37) + i0.042(3)$	- + $i0.063(29)$	/16/
$^{12}\text{C}$	$-0.473(5) + i0.113(6)$	- + $i0.432(41)$	/13/
	- -	$2.330(120) + i0.508(81)$	/14/
$^{16}\text{O}$	$-0.588(4) + i0.151(6)$	- + $i0.425(32)$	/15/
	- -	$2.656(46) + i0.597(32)$	/14/

We present in table 2 the values for  $a_{0,1}^{\text{exp}}$  obtained by (3.1) using the experimental data for  $c_{nl}$  and  $\Gamma_{nl}$  from table 1.

The other way of determining  $a_{0,1}^{\text{exp}}$  consists in using the optical potential which fits the shifts and widths of the pionic atom levels of the nucleus. By this method the following values for the scattering lengths have been obtained <sup>/20/</sup>

$$a_0(^4\text{He}) = (-0.139 + i0.042) \text{ fm}, \quad a_0(^{12}\text{C}) = (-0.452 + i0.132) \text{ fm}, \\ a_0(^{16}\text{O}) = (-0.547 + i0.154) \text{ fm}. \quad (3.3)$$

Practically the same value for  $a_0(^{16}\text{O})$  has been obtained in ref./15/. In refs./15, 20/ the scattering volumes have not been calculated. Comparing (3.3) with the values listed in table 2, we conclude that a simple formula (3.1) well reproduces the results of the optical model calculations.

### 3.2. Scattering lengths and volumes: calculations

We present in table 3 the values for  $a_{0,1}^{\text{pot}}$  calculated in the UST-approach. Two lowest terms in the series were taken into account. In the calculations we use the  $\pi\text{N}$  phase shifts of ref./10/. The errors shown in brackets come from the errors in the  $\pi\text{N}$  data.

Table 3. Pion-nucleus scattering lengths and volumes: potential calculations

Nucleus	$a_0^{\text{pot}}, \text{fm}$	$a_1^{\text{pot}}, \text{fm}^3$
$^4\text{He}$	-0.091(17)	1.058(144)
$^{12}\text{C}$	-0.317(51)	3.215(426)
$^{16}\text{O}$	-0.431(68)	4.240(630)

In fig.1 we compare our results for scattering lengths with the results of other calculations/21-23/ obtained by using both the multiple scattering series /21, 22/ and the Schwinger-like variational method/23/. In fig.1  $a_0^{\text{pot}}$  is presented as a function of the  $\pi\text{N}$  isoscalar scattering length  $b_0 = (\alpha_{11}^0 + 2\alpha_{31}^0)/3$  where  $\alpha_{2I, 2j}^l$  is the  $\pi\text{N}$  scattering lengths. We observe an approximate linear dependence of  $a_0^{\text{pot}}$  with respect to  $b_0$

$$a_0^{\text{pot}}(b_0) = a_0(b_0=0) + A b_0.$$

Up to now there is a substantial uncertainty in the  $\pi\text{N}$  data for  $b_0$  /10, 24/. Thus it is advantageous to get an additional information from the analysis of the low-energy scattering data.

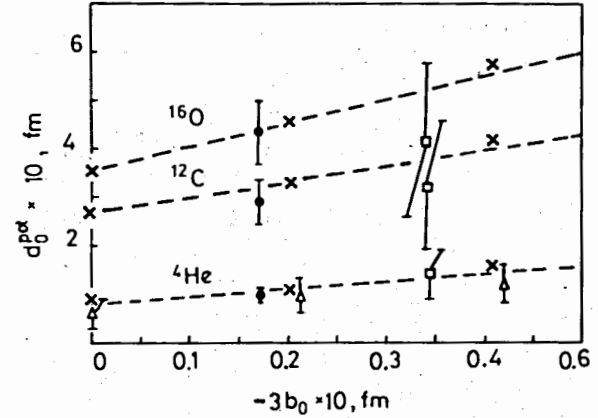


Fig.1 Pion-nucleus scattering lengths  $a_0^{\text{pot}}$  for  $^4\text{He}$ ,  $^{12}\text{C}$  and  $^{16}\text{O}$ .

The black circles are the results of the present paper, the triangles - ref./21/, the squares - ref./22/ and the crosses - ref./23/.

The variational approach /23/ provides summation of the pion rescatterings at all orders. Good agreement of the multiple scattering results with those of variational calculations (at the same values for  $b_0$ ) shows that the multiple scattering series is rapidly convergent not only for  $^4\text{He}$  but also for nuclei with  $A \leq 16$ . Unlike to the scattering lengths  $a_0^{\text{pot}}$ , the scattering volumes  $a_1^{\text{pot}}$  are mainly determined by the first-order term.

### 3.3. Absorption parameters

The imaginary parts of the absorption parameters  $\tilde{B}_0$  and  $\tilde{C}_0$  are determined by (2.4) through the experimental values on  $\text{Im}a_{0,1}$  in a straightforward way. Using the values from table 2, we obtain for  $\text{Im}\tilde{B}_0$  and  $\text{Im}\tilde{C}_0$  the results listed in table 4. We see that within the error limits

$$\text{Im}\tilde{B}_0 = 0.1 \text{ fm}^4 \quad \text{and} \quad \text{Im}\tilde{C}_0 = 1.0 \text{ fm}^6. \quad (3.4)$$

Only for  $^4\text{He}$  the value for  $\text{Im}\tilde{C}_0$  is about twice smaller. As it has been noted above, the experimental value for  $\Gamma_{2p}$  (see table 1) is

Table 4. Imaginary parts of the absorption parameters

Nucleus	$\text{Im}\tilde{B}_0, \text{fm}^4$	$\text{Im}\tilde{C}_0, \text{fm}^6$	Refs.
$^4\text{He}$	0.104(7)	0.442(81)	/16/
$^{12}\text{C}$	0.098(5)	1.081(68)	/13/
	-	1.292(135)	/14/
$^{16}\text{O}$	0.097(4)	0.820(46)	/15/
	-	1.074(46)	/14/

considered as an estimation. Below we shall show that the low-energy scattering data for  $\pi^-^4\text{He}$  are well described using  $\text{Im}\tilde{C}_0=1.0\text{fm}^6$ , as well.

The values for  $\text{Re}\tilde{B}_0$  and  $\text{Re}\tilde{C}_0$  in table 5 are calculated using the values for  $a_{0,1}^{\text{exp}}$  and  $a_{0,1}^{\text{pot}}$  from tables 2 and 3. From eqs.(2.4) it follows that  $\text{Re}\tilde{B}_0$  and  $\text{Re}\tilde{C}_0$  are determined by the difference of  $\text{Re}a_{0,1}^{\text{exp}}$  and  $\text{Re}a_{0,1}^{\text{pot}}$ . It brings about large uncertainties in the values of  $\text{Re}\tilde{B}_0$  and  $\text{Re}\tilde{C}_0$ , caused by the errors in both the pionic atom data and the  $\pi\text{N}$  data. In the next section we shall show that the low energy scattering data can help us to determine more exactly these quantities.

From table 5 it follows that the parameter  $\text{Re}\tilde{B}_0$  is approximately the same for the considered nuclei, and within the error limits, we obtain

$$\text{Re}\tilde{B}_0 = -\text{Im}\tilde{B}_0 = -0.1\text{fm}^4. \quad (3.5)$$

Table 5. Real parts of the absorption parameters

Nucleus	$\text{Re}\tilde{B}_0, \text{fm}^4$	$\text{Re}\tilde{C}_0, \text{fm}^6$	Refs.
$^4\text{He}$	-0.124(101)	-	/16/
$^{12}\text{C}$	-0.136(46)	-2.291(738)	/13,14/
	-0.101(43)	-3.082(904)	/14,15/

Relation of this kind between the real and imaginary parts of the s-wave absorption parameters is usually used in the optical model analysis of pionic atom data<sup>/25/</sup>.

As for  $\tilde{C}_0$ , we obtain the value for  $\text{Re}\tilde{C}_0$  (see table 5) which is approximately three times larger than its imaginary parts. In many optical model analyses the real part of the p-wave absorption parameter  $C_0$  is assumed to be zero, and a good fit of the pionic atom data is then achieved by varying the other parameters of the optical potential, in particular, the parameter  $\xi$  of the LLEE-correction<sup>/25,26/</sup>. In refs.<sup>/27/</sup> a strong correlation between  $\text{Re}\tilde{C}_0$  and  $\xi$  has been demonstrated. In the present approach we use fairly long range  $\pi\text{N}$  interactions (2.3) which suppress the effect of the short range NN correlations (through the LLEE-effect). Thus, as in many optical model analyses presented in the momentum space<sup>/28-32/</sup>, we neglect the LLEE correction.

#### 4. Pion-nucleus scattering: results and discussion

In this section we present the results of our study of low energy pion scattering by  $^4\text{He}$ ,  $^{12}\text{C}$  and  $^{16}\text{O}$ . We shall keep, as a first approximation, the absorption parameters at their pionic

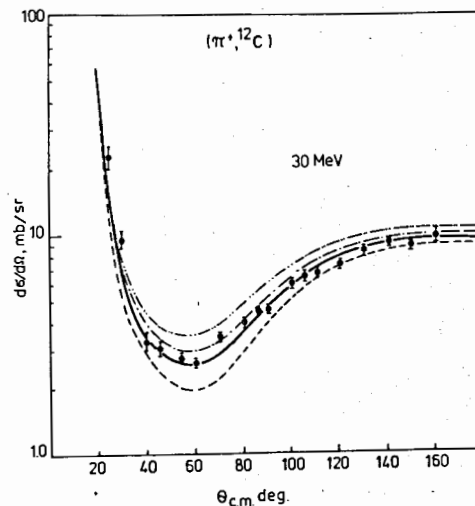


Fig.2. Differential cross section for  $\pi^+ -^{12}\text{C}$  at 30 MeV. The solid curve is calculated for  $\text{Re}\tilde{B}_0 = -0.1 \text{fm}^4$ ; the dashed, dash-dotted and dash-double-dotted lines are for  $\text{Re}\tilde{B}_0 = -0.02, -0.014$  and  $-0.2 \text{fm}^4$ , respectively. The data are from ref.<sup>/33/</sup>.

atom values, and determine the energy range of this approximation by comparing the calculated cross sections with the data.

As it has been shown in the previous section, the real parts of the absorption parameters  $\text{Re}\bar{B}_0$  and  $\text{Re}\bar{C}_0$  are determined with large uncertainties (see table 5). The sensitivity of differential cross sections to variations of these parameters are shown in figs. 2 and 3. We consider here the case of  $\pi^{-12}\text{C}$  scattering at 30 MeV because at the pion energies below this value the sensitivity of the cross sections to the other important parameter of the present approach  $\Lambda$  is negligible ( see figs. 4 and 5 ). From fig.2 it is seen that a good description of the data is achieved at the value of  $\text{Re}\bar{B}_0$  prescribed by relation (3.5). However, the 30% variations around  $-0.1 \text{ fm}^4$  cannot be excluded.

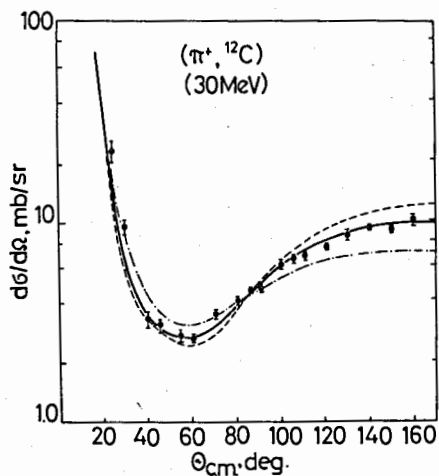


Fig.3. Differential cross section for  $\pi^+ -^{12}\text{C}$  at 30 MeV. The solid curve is calculated for  $\text{Re}\bar{C}_0 = -2.8 \text{ fm}^6$ ; the dashed and the dash-dotted lines are for  $\text{Re}\bar{C}_0 = -2.0$  and  $-4.0 \text{ fm}^6$ , respectively. The data are from ref./33/.

The value  $-0.02 \text{ fm}^4$  of  $\text{Re}\bar{B}_0$  is obtained if the Koch and Pietarinen  $\pi\text{N}$  data /24/ ( $b_0 = -0.014 \text{ fm}$  (or  $-9.7 \times 10^{-3} \text{ m}_\pi^{-1}$ ) ) for calculation  $a_0^{\text{pot}}$  are used. Thus, one can conclude that the low-energy scattering data are compatible with smaller value for  $b_0 = -0.005 \text{ fm}$  (or  $-3.6 \times 10^{-3} \text{ m}_\pi^{-1}$ ) of ref./10/.

The sensitivity of the cross sections to  $\text{Re}\bar{C}_0$  is more pronounced. From fig.3 we obtain that the most appropriate value

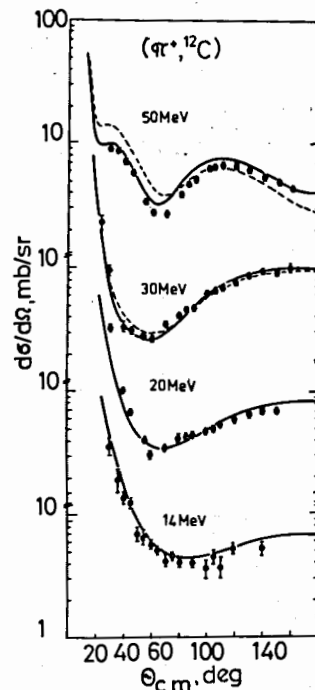


Fig.4. Elastic scattering of  $\pi^+$  at 14, 20, 30 and 50 MeV. The data at 14 MeV are from ref./34/, at 20 MeV - ref./36/, and at 30 and 50 MeV - ref./33/. The solid and dashed curves are calculated for  $\Lambda = 25$  and  $5 \text{ MeV}$ , respectively.

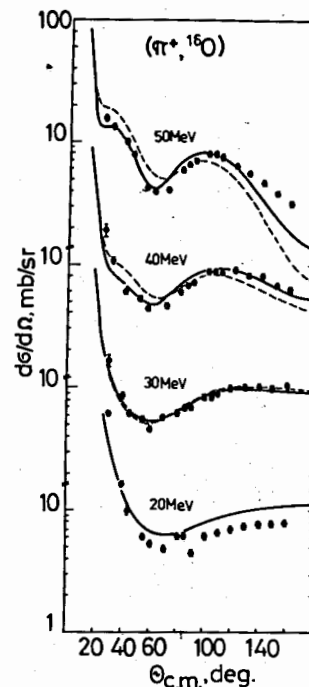


Fig.5. Elastic scattering of  $\pi^+$  from  $^{16}\text{O}$ . The data are from refs./33,35,36/. The sense of the curves is the same as in fig.4.

for this parameter is  $-2.8 \text{ fm}^6$ . The same results are obtained from the analysis of the  $\pi^{16}\text{O}$  data. Therefore, both the pionic atom data and scattering data at energies below 30 MeV are compatible with the following absorption parameter set

$$\begin{aligned} \bar{B}_0 &= (-0.1 + i 0.1) \text{ fm}^4 = (-0.25 + i 0.25) \text{ m}_\pi^{-4} \\ \bar{C}_0 &= (-2.8 + i 1.0) \text{ fm}^6 = (-0.35 + i 0.13) \text{ m}_\pi^{-6} \end{aligned} \quad (4.1)$$

The only parameter which is not still defined is the nuclear mean excitation energy parameter  $\Lambda$ . Below, it is shown (see also ref./5/) that the best description of the scattering data both for  $^{12}\text{C}$  and  $^{16}\text{O}$  is provided by  $\Lambda = 15 - 25 \text{ MeV}$ .



#### 4.1. Differential cross sections

4.1.1.  $^{12}\text{C}$  and  $^{16}\text{O}$ . In figs.4 and 5 we present the results of our calculations of the differential cross sections for the  $\pi^+$  elastic scattering by  $^{12}\text{C}$  and  $^{16}\text{O}$  along with the data from refs.<sup>/33-36/</sup>.

The difference between the solid and the dashed lines shows sensitivity to the parameter  $\Delta$ : the solid lines correspond to  $\Delta=25$  MeV; and the dashed lines, to  $\Delta=5$  MeV. We see that a better description of the data around 50 MeV is obtained for  $\Delta \sim 20$  MeV both for  $^{12}\text{C}$  and  $^{16}\text{O}$ .

The sensitivity to  $\Delta$  is more pronounced at energies around 50 MeV and becomes weaker when the energy of a pion decreases. It

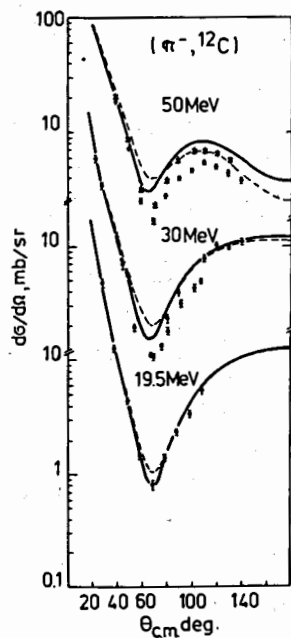


Fig.6. Elastic scattering of  $\pi^-$  from  $^{12}\text{C}$  at 20, 30 and 50 MeV. The sense of the curves is the same as in fig.4. The triangles label the data from ref.<sup>/6/</sup>, the black circles - ref.<sup>/7/</sup>, the crosses - ref.<sup>/37/</sup>.

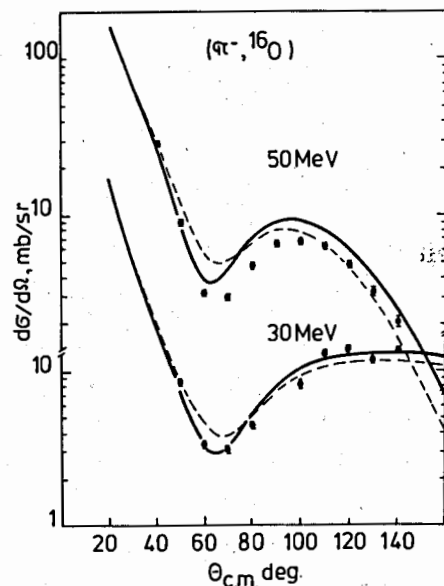


Fig.7. Elastic scattering of  $\pi^-$  from  $^{16}\text{O}$  at 30 and 50 MeV. The sense of the curves is the same as in fig 4. the data are from ref.<sup>/7/</sup>.

reflects a dominance of the pion absorption correction at energies below 30 MeV in the formation of the inelasticity parameters. At energies around 50 MeV the differential cross sections arise as a result of strong interference between the absorption channel and the pure potential channels (see below subsect. 4.1.3).

In figs.6 and 7 we compare the results of our calculations for the  $\pi^-$  scattering with the experimental data <sup>/6,7,37/</sup>. The calculated differential cross sections at 50 MeV overestimate appreciably the recent data of ref.<sup>/7/</sup> at large angles and are in good agreement with the older data obtained in ref.<sup>/37/</sup>. Moreover, we obtain a very good description of the asymmetry parameter  $A(\theta)$  (see fig.8)

$$A(\theta) = (d\sigma^-/d\Omega - d\sigma^+/d\Omega) / (d\sigma^-/d\Omega + d\sigma^+/d\Omega)$$

for the  $\pi^\pm - ^{12}\text{C}$  data of ref.<sup>/37/</sup> at 50 MeV.

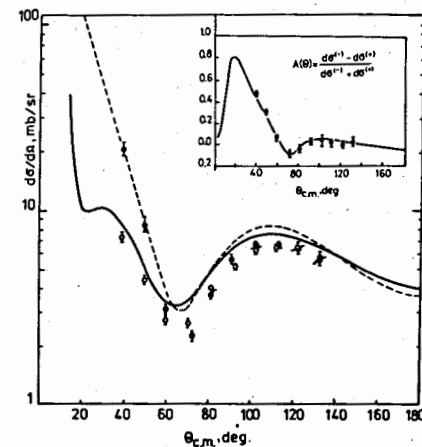


Fig.8. Differential cross sections and angular dependence of the asymmetry parameter for  $\pi^\pm - ^{12}\text{C}$  at 50 MeV. The data are from ref.<sup>/37/</sup>. The curves are calculated for the parameter set (4.1) and  $\Delta=25$  MeV.

4.1.2.  $^4\text{He}$ . In figs 9 and 10 we present the calculated differential cross sections of  $\pi^\pm - ^4\text{He}$  scattering along with the data from refs.<sup>/38-41/</sup>. In the calculations we use the same absorption parameter set (4.1) as for  $^{12}\text{C}$  and  $^{16}\text{O}$ , and the solid lines correspond to  $\Delta = 21$  MeV which is the first excited state of  $^4\text{He}$ . Hence, without any free parameters we obtain a good description of the scattering data in the energy domain 0 - 50 MeV.

It can be shown that one cannot describe well the  $\pi^\pm - {}^4\text{He}$  differential cross sections using  $\text{Im}\bar{C}_0$  consistent with the value of  $\Gamma_{2p}$  from ref./16/. Thus, it is profitable to determine the values of both the shift and width in the 2p-level of pionic helium which are consistent with the parameter set (4.1).

Substituting (4.1) and the value for  $a_1^{\text{pot}}$  from table 3 into eqs.(2.4) we obtain

$$a_1^{\text{exp}} = (-0.689 + i0.136) \text{ fm}^3. \quad (4.2)$$

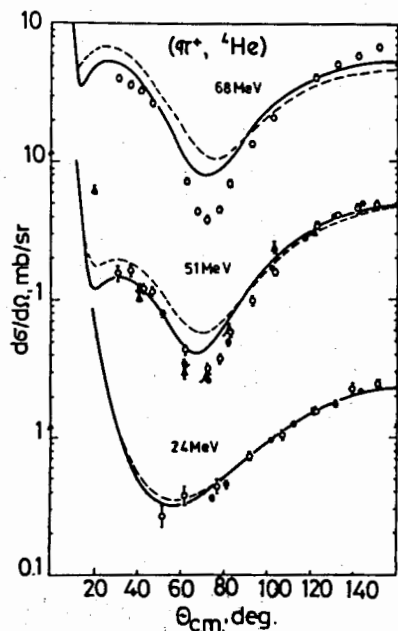


Fig.9. Elastic scattering of  $\pi^+$  from  ${}^4\text{He}$  at 24, 51 and 68 MeV. The solid and dashed curves are calculated for  $\Delta = 21$  and 5 MeV, respectively. The open circles label the data from refs./38,40/, the black circles - ref./39/ and the triangles - ref./41/.

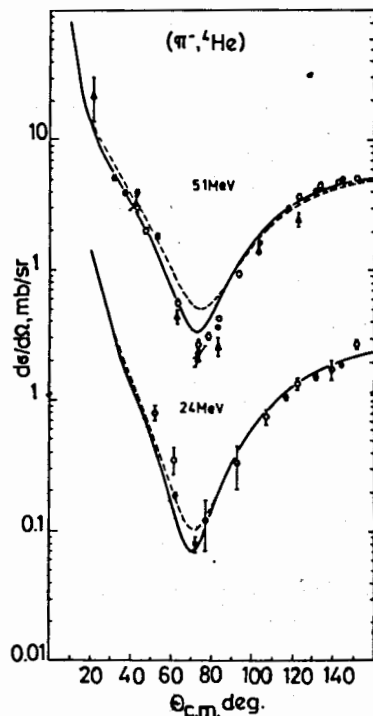


Fig.10. The same as in fig.9, but for  $\pi^- - {}^4\text{He}$ .

Finally, using the DGBT-formula (3.1) we obtain the following strong interaction shift and width in the 2p-level

$$e_{2p} = 4.0 \times 10^{-3} \text{ eV} \quad \text{and} \quad \Gamma_{2p} = 1.6 \times 10^{-3} \text{ eV}. \quad (4.3)$$

The obtained value for  $\Gamma_{2p}$  is approximately twice the experimental result of ref./16/ and is compatible with the earlier result of ref./42/ :  $\Gamma_{2p} = (2.0 \pm 1.3) \times 10^{-3} \text{ eV}$ . For the ratio  $\Gamma_{2p}/\Gamma_{1s}$  we obtain

$$\Gamma_{2p}/\Gamma_{1s} = 3.6 \times 10^{-3}.$$

This value is in good agreement with the Hüfner estimation /25/ :  $3 \times 10^{-3}$ .

In our earlier paper/11/, we used the absorption parameter set:  $\bar{B}_0 = (-0.153 + i0.109) \text{ fm}^4$  and  $\bar{C}_0 = (-5.538 + i1.136) \text{ fm}^6$ . These values are obtained if in the calculations of the potential parts of the  $\pi$ -nucleus phase shifts  $\delta_{\pi A}^{\text{pot}}$  the pole part of the  $\pi N$   $p_{11}$ -wave is subtracted. The description of the scattering data obtained here is better than in /11/. It supports the conclusion ( see Part 1) that if a local density approximation is used for calculating  $\delta_{\pi A}^{\text{abs}}$ , the subtraction procedure is not needed.

4.1.3. Effect of pion absorption. The results of our calculation presented in fig.11 (see also refs./5,11/) show a strong influence of the pion absorption on the elastic scattering at low energies. The pion absorption reduces the differential cross section at both the forward and backward angles. The same effect has been observed for the  $\pi$ -d scattering in ref./43/. Switching on the absorption decreases the total elastic cross section approximately twice at 50 MeV. Hence, we can conclude that around 50 MeV the differential cross sections arise as a result of strong interference between the pure potential and the absorption channels. At energies below 30 MeV the total reaction cross section is formed mainly by pion absorption channel.

Our conclusion about the role of the pion absorption at low energies diverges strongly from that given by Landau and Thomas (LT) in ref./28/. From their calculations it follows that at low

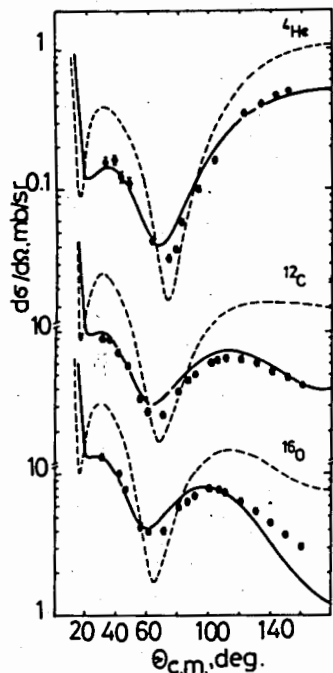


Fig.11. Elastic scattering of 50 MeV  $\pi^+$  from  $^4\text{He}$ ,  $^{12}\text{C}$  and  $^{16}\text{O}$ . The data are from refs./33,40/. The dashed curves represent the result of pure potential calculations and the solid curves include the effect of absorption.

energies the pion absorption systematically raises the differential cross sections (see figs 9 and 10 in /28/), and the role of the pion absorption is mainly reduced to fill the minima in the differential cross sections.

Let us compare in more detail the results of our calculations with those of LT for the  $\pi^{-12}\text{C}$  scattering at 50 MeV. Our results of pure potential calculations of the s- and p-wave phase shifts ( $\delta_l^{\text{pot}} \equiv \text{Re} \delta_{\pi A, l}^{\text{pot}}$ ) are:  $\delta_0^{\text{pot}} = -12^\circ$  and  $\delta_1^{\text{pot}} = 25^\circ$  (see table 1 in Part 1), while the LT results are:  $\delta_0^{\text{pot}} = -3^\circ$  and  $\delta_1^{\text{pot}} = 15^\circ$  (see table 3 in /28/). This difference makes it clear why our potential calculations overestimate the  $\pi$ -nucleus differential cross sections and those of LT underestimate them. We believe that our results are correct for several reasons. First, our calculations have been made within the range of convergence of the iterative series (in /28/ the first-order optical potential has been used). Second, we obtain for the  $\pi^{-4}\text{He}$  scattering at 50 MeV

the following results:  $\delta_0^{\text{pot}} = -7.5^\circ$  and  $\delta_1^{\text{pot}} = 13^\circ$  which are in good agreement with the optical model calculations of Mach and Sapozhnikov /44/ (second-order optical potential):  $\delta_0^{\text{pot}} = -6.5^\circ$  and  $\delta_1^{\text{pot}} = 11^\circ$ . Therefore, it would be surprising if one gets for  $\pi^{-12}\text{C}$  the phase shifts which are smaller than those in the  $\pi^{-4}\text{He}$  case. Finally, after the inclusion of the pion absorption correction with the set of parameters (4.1), we obtain the phase shifts:  $\delta_0 = -17.2^\circ$  and  $\delta_1 = 14^\circ$ , which are in good agreement with the results of the phase shift analysis of the  $\pi^{-12}\text{C}$  scattering data /45/:  $\delta_0 = -17.1^\circ$  and  $\delta_1 = 13^\circ$  while the LT results for the phase shifts after the inclusion of the pion absorption are:  $\delta_0 = -6.6^\circ$  and  $\delta_1 = 15.5^\circ$ .

The values of the absorption parameters used in the LT calculation were taken from the pionic atom fits made with the Kissinger-like potential (see, e.g. ref./25/). It is known that the values of these parameters depend strongly on the form of the optical potential. In particular, the value of  $\text{Re} C_0$  is correlated with the value of the parameter  $\xi$  of the LEE-effect (see, e.g. /25,27/). Therefore, to determine the absorption parameters of the given optical potential self consistently, one should make the pionic atom fits using this potential.

In fig.12 we show the energy dependence of the pion-nucleus phase shifts and inelasticity parameters for  $\pi^{-12}\text{C}$ . The same picture is observed for the  $\pi^{-16}\text{O}$  scattering. The obtained energy dependence is in good agreement with the PSA data of refs./45/.

## 7.2 Total cross sections

Using the optical theorem one can calculate the total ( $\sigma_{\text{tot}}$ ) and the total reaction ( $\sigma_{\text{R}} = \sigma_{\text{tot}} - \sigma_{\text{el}}$ ) cross sections. It is also possible to estimate the total absorption cross section ( $\sigma_{\text{abs}}$ ) by switching off the potential part ( $\delta^{\text{pot}}$ ) of the pion-nucleus phase shifts. The energy dependence of  $\sigma_{\text{tot}}$ ,  $\sigma_{\text{el}}$  and  $\sigma_{\text{abs}}$  for the pion

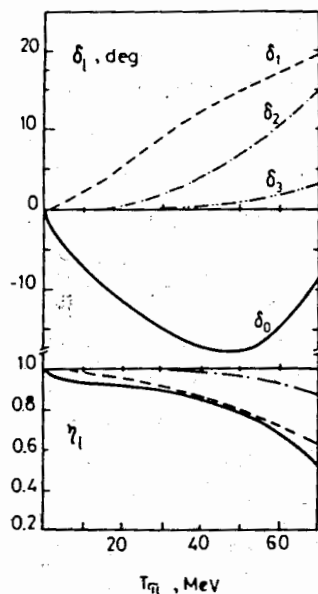


Fig.12. Pure hadronic phase shifts and inelasticity parameters for  $\pi - {}^{12}\text{C}$ .

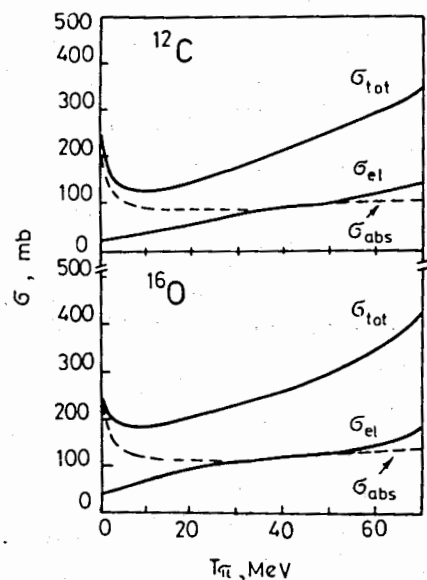


Fig.13. The total, total elastic and total absorption cross sections for  $\pi - {}^{12}\text{C}$  and  ${}^{16}\text{O}$  versus the pion energy (in the lab.)

scattering by  ${}^{12}\text{C}$  and  ${}^{16}\text{O}$  is shown in fig.13. The calculations are performed for  $\Delta = 20$  MeV. We see that  $\sigma_{\text{abs}}$  is practically energy independent in the considered energy range, and  $\sigma_{\text{abs}} \approx 100$  mb and 120 mb for  ${}^{12}\text{C}$  and  ${}^{16}\text{O}$ , respectively. At energies around 50 MeV  $\sigma_{\text{inel}} = \sigma_{\text{tot}} - \sigma_{\text{el}}$  estimated by setting  $\delta^{\text{abs}} = 0$  becomes comparable with  $\sigma_{\text{abs}}$ , which shows the beginning of the interference between the pure potential and the absorption channels. The same results for the pion- ${}^4\text{He}$  scattering have been obtained in ref./11/.

In ref./5/ the sensitivity of  $\sigma_{\text{tot}}$  on the parameter  $\Delta$  has been investigated for  $\pi - {}^{12}\text{C}$  and  $\pi - {}^{16}\text{O}$  at 50 MeV. Comparing the calculated and the experimental values of  $\sigma_{\text{tot}}$ , it was shown that, as for the differential cross sections, the most appropriate

range for  $\Delta$  is 15 - 25 MeV. The experimental values for  $\sigma_{\text{tot}}$  have been estimated using the interpolating formula obtained in ref./46/.

Quite recently first results on the total reaction cross sections for the  $\pi^{\pm}$  mesons on a considerable number of nuclei have been obtained /8/. For  ${}^{12}\text{C}$   $\sigma_{\text{R}}^{\pm}$  has been measured at 50 and 65 MeV, and for  ${}^{16}\text{O}$  at 50 MeV. Preliminary data on  $\sigma_{\text{R}}^{\pm}$  for the  $\pi^{\pm} - {}^{12}\text{C}$  scattering reported in /47/ agree well with the results of ref./8/. In table 6 we present the calculated values of  $\sigma_{\text{R}}$  along with the experimental data. We see that the calculated cross sections for the  $\pi^{\pm}$  mesons are in agreement with the data for  $\Delta = 15 - 20$  MeV. Some underestimation is observed for  $\pi^{-}$ . Thus, the experimental data show a more stronger Coulomb effect than it is obtained in the calculations.

Table 6. Total reaction cross sections ( $\sigma_{\text{R}}^{\pm} = \sigma_{\text{tot}}^{\pm} - \sigma_{\text{el}}^{\pm}$ ) for  $\pi^{\pm} - {}^{12}\text{C}$  and  ${}^{16}\text{O}$  at 50 and 65 MeV versus the parameter  $\Delta$

$T_{\pi}$ , MeV	Nucleus	$\sigma_{\text{R}}^{\pm}$ , mb	Theory: $\Delta$ , MeV			Exp./8/
			15	20	25	
50	${}^{16}\text{O}$	$\sigma_{\text{R}}^{+}$	175	163	153	$166 \pm 19$
		$\sigma_{\text{R}}^{-}$	216	201	188	$242 \pm 21$
	${}^{12}\text{C}$	$\sigma_{\text{R}}^{+}$	144	134	125	$150 \pm 16$
		$\sigma_{\text{R}}^{-}$	171	160	149	$193 \pm 10$
65	${}^{12}\text{C}$	$\sigma_{\text{R}}^{+}$	192	180	168	$201 \pm 16$
		$\sigma_{\text{R}}^{-}$	220	206	193	$251 \pm 20$

### 5. Conclusion

It has been shown that both the pionic atom data and the low energy pion scattering data for the nuclei  ${}^4\text{He}$ ,  ${}^{12}\text{C}$ , and  ${}^{16}\text{O}$  can be described using the same set (4.1) of the absorption

parameters. The calculated pion-nucleus phase shifts are in good agreement with the results of the phase shift analysis from refs.<sup>/45/</sup>. We obtained that the absorption parameters can be considered as to be constant in the energy range from 0 to 50 MeV. This confirms the dominance of the pion absorption by two close correlated nucleons.

Taking into account that this parameter set provides a good description of the  $\pi^{\pm}$  -<sup>4</sup>He scattering data, and the value for  $\bar{B}_0$  is consistent with the data on the pionic helium 1s-energy level shift and width, we determined the width and shift in the 2p-energy level of pionic helium. The obtained values are:  $c_{2p} = 4.0 \times 10^{-3}$  eV and  $\Gamma_{2p} = 1.6 \times 10^{-3}$  eV.

Our conclusion about the influence of the pion absorption on the elastic scattering quantitatively strongly differs from that demonstrated by Landau and Thomas in their paper <sup>/28/</sup>. We showed that at energies around 50 MeV the differential cross sections arise as a result of strong interference between the pure potential effects and pion absorption channel. At energies below 30 MeV the inelasticity parameters are formed mainly by the absorption channel.

The effect of interference makes the scattering data to be very sensitive to the mechanism of the pion-nucleus interaction. In particular, it becomes possible to determine the only free parameter of the theory  $\Lambda$  which is a certain mean excitation energy of a nucleus. We obtained that for the p-shell nuclei the best description of the data is provided by  $\Lambda = 15-25$  MeV. Unfortunately, accuracy of the recent data <sup>/8/</sup> on the total reaction cross sections on  $\pi$  -<sup>12</sup>C and <sup>16</sup>O at 50 and 65 MeV does not allow to narrow the uncertainty in the value of  $\Lambda$ .

Taking into account that in the p-shell nuclei (see refs.<sup>/48/</sup>) the excitation spectra show a pronounced giant resonance structure concentrated around 20-30 MeV, it is natural to suppose that the

$\approx 20$  MeV value for  $\Lambda$  reflects the dominant role of the nuclear resonance mechanism in the formation of the pion-nucleus parameters. As for the  $\pi$ -<sup>4</sup>He case, this value of  $\Lambda$  coincides with the first excited state of <sup>4</sup>He. Along this line we come to the model of two energy levels of a nucleus for the description of the pion-nucleus interaction.

In the present paper, in the framework of the UST-approach we analysed the pion interaction with light nuclei and at low energies because of convergence of the considered iteration scheme of solving the basic equations. To extend this consideration to the case of more heavier nuclei and to higher energies it is necessary to develop noniterative methods of solving the basic equations and to determine the energy dependence of the absorption parameters. Nevertheless, we believe that the main features of the pion-nucleus dynamics at low energies which have been found in the present study are also valid for more heavier nuclei.

The author is indebted to V. B. Belyaev, R. A. Eramzhyan, D. A. Kirzhnits and R. Mach for stimulating discussions and helpful advices. He also wishes to thank to A. P. Sapozhnikov for the help in the numerical calculations, and to B. Kämpfer for suggestions concerning the manuscript.

#### References

1. Khankhasayev M. Kh., JINR E4-89-443, Dubna, 1989.
2. Khankhasayev M. Kh., Yad.Fiz., 1982, 36, 633; ibid., 1983, 37, 1196
3. Khankhasayev M. Kh., Fiz. Elem. Chastits At. Yadra, 1985, 16, 1223
4. Kirzhnits D. A., JETP, 1965, 49, 1544; Kirzhnits D. A., Krjuchkov G. Yu., Takibaev N. Zh., Fiz. Elem. Chastits At. Yadra, 1979, 10, 741
5. Khankhasayev M. Kh., Sapozhnikov A. P., Phys. Lett. B, 1988, 201, 17
6. Wright D. H., et. al., Phys. Rev. C, 1987, 36, 2139

7. Seth K. K., et. al., Phys. Rev. C (to be published )
8. Meirav O., et. al., Phys. Rev. C, 1987, 36, 1066
9. Sick J., McCarthy J. S., Nucl. Phys. A, 1970, 150, 631;  
Frosch R. F., et al., Phys. Rev., 1967, 160, 874
10. Row G., Solomon M., Landau R. H., Phys. Rev. C, 1978, 18, 584
11. Belyaev V. B., Khankhasayev M. Kh., Phys. Lett. B, 1984, 137, 299
12. Bebeck G. J., et. al., Phys. Rev. D, 1978, 17, 1693
13. Fry C. A., et. al., Nucl. Phys., 1982, A 375, 325
14. De Chambrier G., et. al., Nucl. Phys. A, 1985, 442, 647
15. Swanner J., et. al., Nucl. Phys. A, 1984, 412, 253
16. Backenstoss G., et. al., Nucl. Phys., 1974, A 232, 519
17. Dezer S., Goldberger M. L., Baumann K., Thirring W., Phys. Rev. 1954, 96, 774
18. Backenstoss G., Ann. Rev. Nucl. Sci., 1970, 20, 467
19. Seki R., Phys. Rev., 1969, 182, 1773
20. Hüfner J., Tauscher L., Wilkin C., Nucl. Phys. A, 1974, 231, 455
21. Lohs K. P., Nucl. Phys. A, 1978, 312, 297
22. Moyer L., Koltun D. S., Phys. Rev. 1969, 182, 999
23. Belyaev V. B., Zubarev A. L., Rahimov A. A., Journ. Phys. G., 1980, 6, L 49; Belyaev V. B., Rahimov A. A., JINR report P4-81-672, Dubna, 1981 (in Russian)
24. Koch R., Pietarinen E., Nucl. Phys. A, 1980, 336, 331;  
Dumbras O., et. al., Nucl. Phys. B, 1983, 216, 277
25. Hüfner J., Phys. Reports, 1975, 21C, 1
26. Ericson M., Ericson T. E. O., Ann. of Phys., 1966, 36, 323
27. Seki R., Masutani K., Phys. Rev., 1983, C 27, 2799; Seki R., Masutani K., Yazaki Y., ibid., 1983, C 27, 2817
28. Landau R. H., Thomas A. W., Nucl. Phys., 1978, A 302, 461
29. Mach R., Chech. J. Phys., 1983, 33, 616; Gmitro M., Kvasil J., Mach R., Phys. Rev., 1985, C 31, 1349
30. De Kam J., van Geffen F., van der Velde M., Nucl. Phys. A 1980, 333, 443
31. Liu L. C., Shakin C. M., Progr. Part. Nucl. Phys., 1981, 5, 207
32. Gmitro M., Kamalov S. S., Mach R., Phys. Rev., 1987, C 36, 1105
33. Preedom B. M., et. al., Phys. Rev. C, 1981, 23, 1134
34. Gill D. R., et. al., Phys. Rev. C, 1982, 26, 1306
35. Blecher M., et. al., Phys. Rev. C, 1979, 20, 1884
36. Obenshain F. E., et. al., Phys. Rev. C, 1983, 27, 2753

37. Sobie R. J., et. al., Phys. Rev. C, 1984, 30, 1612
38. Nordberg M. E., Kinsey K. F., Phys. Lett., 1978, 20, 499
39. Fournier G., et. al., Nucl. Phys. A, 1984, 426, 542
40. Crow K. M., et. al., Nucl. Phys., 1969, 180, 1349
41. Källne J., et. al., Phys. Rev. Lett., 1980, 45, 517
42. Berezin S., et. al., Phys. Rev. A, 1970, 2, 1630
43. Afnan I. R., Blankleider B., Phys. Lett. B, 1980, 93, 367;  
Phys. Rev. C, 1980, 22, 1638
44. Mach R., Sapozhnikov M. G., J. Phys. G, 1984, 10, 147
45. Fröhlich J., Schlaile H. G., Streit L., Zingle H., Z. Phys. G, 1981, 302, 89; Dumbras O., Fröhlich J., Klein U., Schlaile H.G., Phys. Rev. C, 1984, 29, 581
46. Carrol A. S., et. al., Phys. Rev. C, 1976, 14, 635
47. Berkhout J. B., et. al., Proc. XI Int. Conf. on Particle and Nuclei, Kyoto, 1987, Abstract Book 1, c-94, p. 394
48. Goncharova N. G., Kissener H.-R., Eramjan R. A., Fiz. Elem. Chastits At. Yadra, 1985, 16, 773; George Mc, et. al., Phys. Lett. B, 1986, 179, 212